The Seismic Source Characteristics In the Alaska Subduction Zone

SE28-A032

Chung-Hung Lo[1*], Ban-Yuan Kuo[2], Justin Yen-Ting Ko[1,3], Ling-Yun Chiao[1]

[1]Geophysics, Institute of Oceanography, National Taiwan University, Taipei, Taiwan [2]Institute of Earth Sciences, Academia Sinica, Taipei, Taiwan [3]California Institute of Technology, Pasadena, California

*Email：r05241304@ntu.edu.tw

Abstract

In this study, we employed a cluster-event method (CEM) to constrain the source parameters as well as along-path attenuation in the Alaska subduction zone. Neighborhood algorithm is applied to solve the nonlinear inverse problem. Using 40 stations from IRIS data management center, we analyzed 144 Alaska local earthquakes spreading over a depth range from 90 to 170 kilometers and a seismic magnitude range from 3 to 5 in 2012~2017. The fc's satisfy a self-similar scaling relationship with seismic moment of fc $\propto M_0{}^{-3}$ with a mean stress drop of 18.34 $\pm$ 1.10 MPa in Madariaga's form (Vs model). The lower radiation efficiency and higher stress drop might imply the shear heating instability as the faulting mechanism for intermediate-depth earthquakes.

Introduction

Corner Frequency (fc) – reflect the seismic source behavior

The fc reflects the source rupture behavior.
It is one of seismic source parameters.
The right cartoon displays an example of the far-field displacement spectrum. (Shearer, P. 2009)

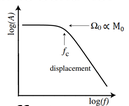

Attenuation (t) – reflect the wave propagation effect*

The t* that affects amplitudes is energy loss due to anelastic processes or internal friction during wave propagation.

$$\frac{1}{Q} \equiv \frac{-\Delta E}{2\pi E} \qquad A(x,T,f) = A_0 e^{-\pi f T/Q} \qquad Q = \frac{T}{t^*}$$

$$t^* = \int \frac{x}{v \cdot Q} \qquad t^* = t_0{}^* f^{-\alpha}$$

x：position T：travel time
f：frequency
α = 0 in this study

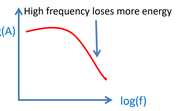

*Trade off issue - fc and t**

The fc and t* effects can be similar in the spectrum and hard to distinguish in the presence of noise. It is a nonlinear inverse problem.

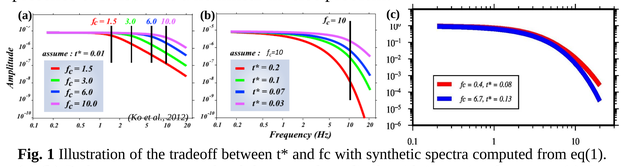

Fig. 1 Illustration of the tradeoff between t* and fc with synthetic spectra computed from eq(1). **(a) (b)** Both parameters act to bend the spectral amplitude with increasing frequency. **(c)** For example, (0.4,0.08) is similar to (6.7,0.13) in the (fc, t*) space.

Brune-type source model

The model spectrum is calculated by 3 parameters (Ω_0, fc, t*). fc and t* were searched by NA. Ω_0 was determined by the mean of low frequencies which can be shifted on the spectrum. (see Fig.4)

$$A(f_i) = \frac{\Omega_0 \exp(-\pi f_i t_j^*)}{1 + (\frac{f_i}{f_{c,k}})^2} \quad \text{eq(1)} \qquad \Omega_0 = C \cdot M_0, \qquad C = \frac{{}_cU_{\phi\theta}}{4\pi\rho v_p^3 R}, \text{ (Brune, 1970)}$$

f_i : frequency
ρ : density of the source material
R : source-receiver distance
Ω_0 : the low frequency asymptote of the spectrum
V_p : P wave velocity near the source
${}_cU_{\phi\theta}$: 0.52 for P, the spherical average of radiation patterns

Methodology

Cluster-Event Method (CEM)

In this study, we apply CEM (*Ko et al., 2012*) to determine fc and t* robustly.

CEM assumption

- The nearby seismic sources are regarded as a cluster.
- All seismic sources in the cluster share the identical attenuation to the same station because of their similar ray-path.
- In the cluster, each event recorded by several stations is allowed only for a single corner frequency.
- CEM ignores site effects and source directivity.

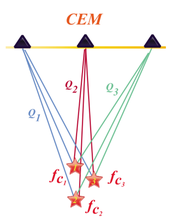

(Ko et al., 2012)

Criteria for the cluster (# of event ≥ 3 and # of station ≥ 3)

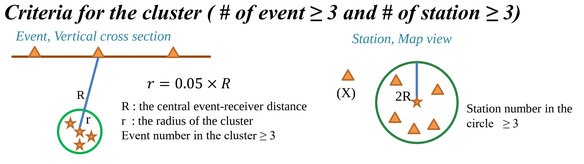

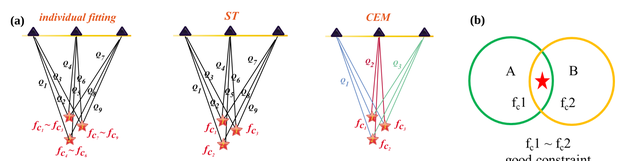

	Individual fitting	ST (Stachnik et al., 2004)	Cluster Event Method
Inverse Dimension	$3(f_c) \times 3(t^*) \times 3 = 27$	$1(f_c) \times 3(t^*) \times 3 = 9$	$3(f_c) + 3(t^*) = 6$

Fig. 2 Comparison of 3 approaches with inverse dimensions for 3 events and 3 stations. **(a)**The CEM suppresses the trade off between fc and t* with much less degrees of freedom to satisfy all the spectrum data. **(b)** Cross-cluster event provides the constraint to CEM.

Neighbourhood Algorithm (NA)

The NA is conceptually simple with at most 2 controlling parameters, but is able to exhibit self-adaptive behavior while seeking a data-acceptable solution in model space. These 2 parameters are ns (the total numbers of new models generated at each iteration) and nr (the number of best fitting regions which the new model can generate). To broaden the survey and to insure the convergence of the algorithm, ns = 500, nr = 100, and 50 iterations are used.

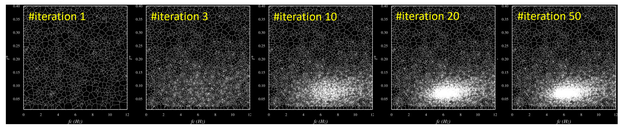

Fig. 3 Five iteration snapshots of the CEM solution for the 2017-03-07.09.50.08-N19K (event-station) pair. The panels from left rightward show the evolution of the CEM solution and the Voronoi cell is used in the NA in the model space.

The misfit of CEM_NA

For example, there are 3 events in the cluster and recorded by 4 stations, and NA generated a model X = $[f_{c,1}\ f_{c,2}\ f_{c,3}\ t_1{}^*\ t_2{}^*\ t_3{}^*\ t_4{}^*]$. The minimum misfit F_{kj} would be calculated for observed spectrum recorded by jth station from the kth event within the cluster (eq(2)). Then, θ (average F) is considered as the total misfit to the model X. Minimum θ is the best model for the cluster.

(a)

$$F_{kj} = \min\left(\frac{\sum_{i=1}^{M} w_i \times \| \frac{\Omega_0 \exp(-\pi f_i t_j^*)}{1 + (\frac{f_i}{f_{c,k}})^2} - d_{kj,i} \|_2}{\sum_{i=1}^{M} w_i}\right) \quad \text{eq(2)}$$

$$\delta_i = |log_{10}(f_{i,signal}) - log_{10}(f_{i,noise})|$$
$$w_i = 0 \quad \delta_i < 0.5 \approx log_{10}(3)$$
$$w_i = 2\delta_i \quad 0.5 \le \delta_i \le 2$$
$$w_i = 4 \quad \delta_i > 2$$

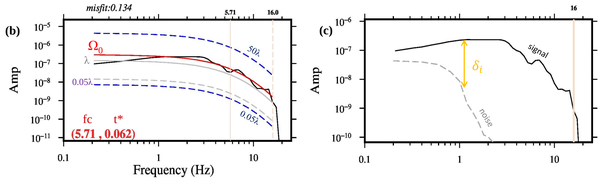

Fig. 4 Illustration of model misfit. **(a)** The misfit function in this study **(b)** Ω_0 determination. 0.05λ : Ω_0 shift interval; λ = the mean of low-frequency (< 1 Hz) in the observed spectrum **(c)** The value of w_i is based on the signal-noise ratio. Blackline : 5 s window of P waveform spectrum. Dash-line: the noise spectrum that 5 s window before and 1 s apart P waveform.

Seismic Data

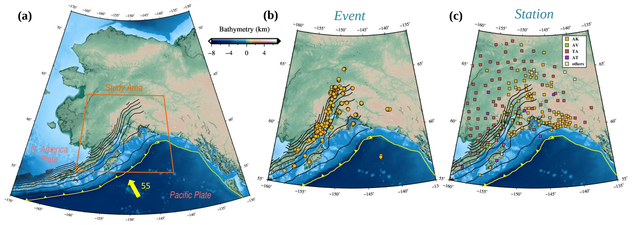

Fig. 5 Data distribution **(a)** Overview of the Alaska subduction zone. **(b)** Events used with the depth 90-170 km, the longitude -142°~ -160°, and the latitude 56° ~ 66°. **(c)** Broadband seismic stations used in this study.

Criteria for the waveform

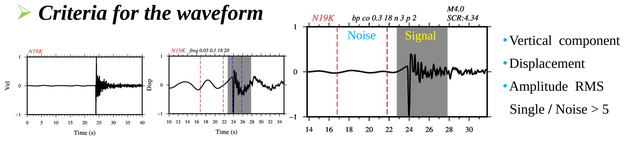

- Vertical component
- Displacement
- Amplitude RMS Single / Noise > 5

*CEM Result - fc & t**

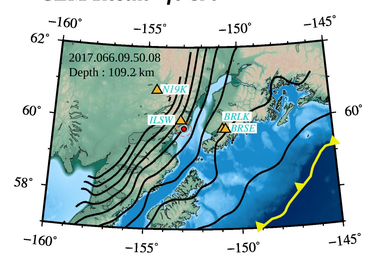

Fig. 9 The result of the CEM inversion. **(a)** Events and stations distribution. The red dot is the example event. **(b) (left)** waveform **(right)** Black line: the signal spectrum. Red line: the model spectrum. **(c)** the global misfit distribution. We calculated the misfit by changing the fc-t* of the target event-station pair and fixed other parameters in the best model. The result show the robustness of fc and t*.

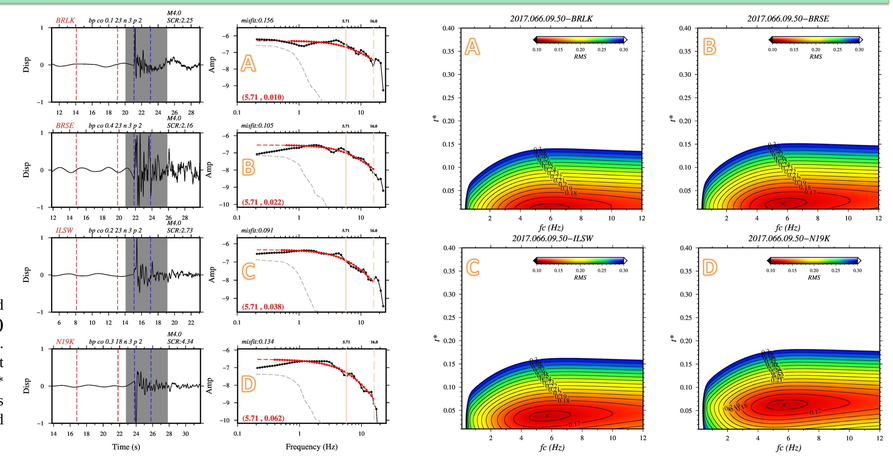

Source Parameters-Depth Relationship and Q

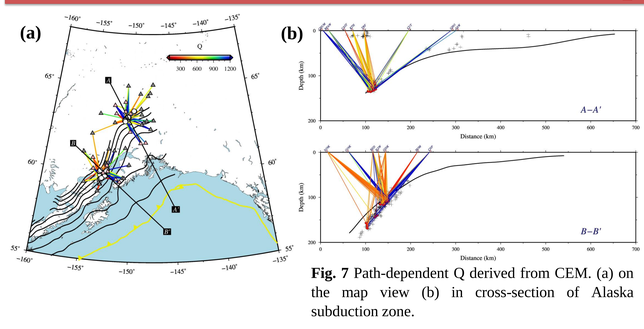

Fig. 7 Path-dependent Q derived from CEM. (a) on the map view (b) in cross-section of Alaska subduction zone.

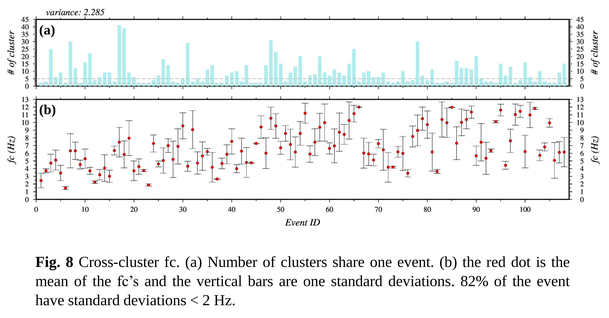

Fig. 8 Cross-cluster fc. (a) Number of clusters share one event. (b) the red dot is the mean of the fc's and the vertical bars are one standard deviations. 82% of the event have standard deviations < 2 Hz.

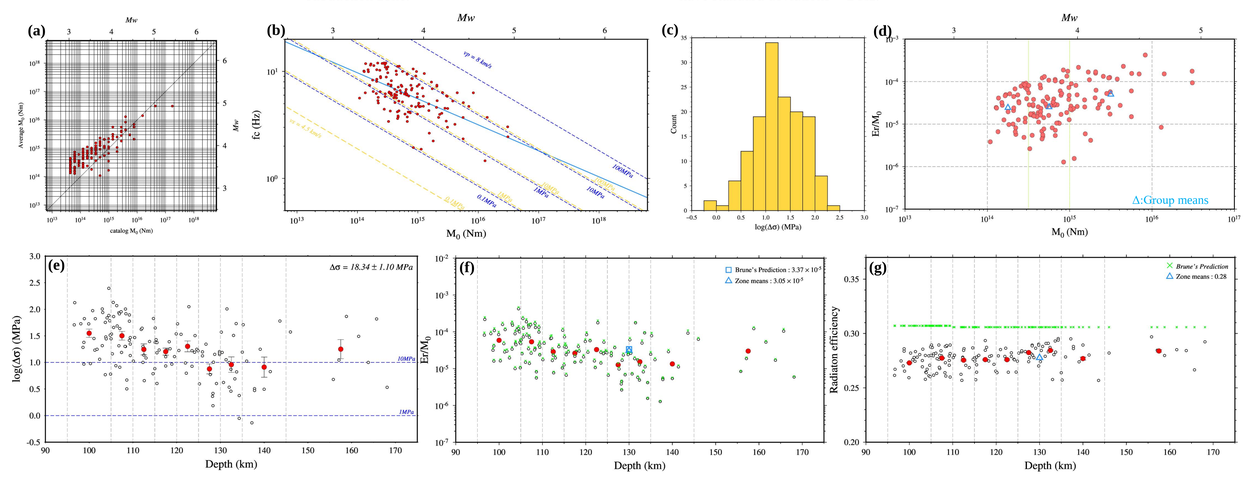

Fig. 10 The relationship between source parameter and depth. **(a)** catalog M_0 versus average M_0. The average M_0 is calculated by Ω_0 for all stations and averaged them for each event. Catalog M_0 is converted by Mw which is estimated by local magnitude. The following M_0 are all average M_0. **(b)** Measured fc versus average M_0. Blue line is the Vp model and gold line is the Vs model. **(c)** Histogram for Δσ (stress drop) are calculated by Vs model. **(d)** Er/M_0 (the scale energy) as a function of M_0. The three moment intervals separated at M_0= $10^{14.5}$ and 10^{15}. The means increase with M_0, but the overall trend is weak. **(e)** Δσ versus depth. Red circles are means (with standard errors) of each 5 km depth interval; if the number of data is less than 10 in an interval, the thickness increments by every 5 km until the number of data is 10 or greater. The all mean and the standard error of Δσ is 18.34 ± 1.10 MPa. **(f)** Er/M_0 as a function of depth. The means predicted by Brune's source model, $(Er/M_0)^B$, is plotted in square, and the measured Er/M_0 is plotted in triangle. Crosses in green are calculated by brune model. **(g)** η_R(Radiation efficiency) as a function of depth. Each data points are in circle. The standard error of the means is shown.

$$E_r = \frac{8\pi}{15\rho\alpha^5}[1 + 1.5(\frac{\alpha}{\beta})^5] \sum f^2 \frac{(\frac{M_0}{1 + (\frac{f}{f_c})^2})^2 \Delta f}{} \quad \text{eq(3)}$$

$$(\frac{E_r}{M_0})^B = \frac{2\pi^2}{15\mu}[1.5 + (\frac{\alpha}{\beta})^5]\frac{16}{7}k^3\,\Delta\sigma \quad \text{eq(4)}$$

$$\eta_R = 2\mu\frac{1}{\Delta\sigma}(\frac{E_r}{M_0}) \quad \text{eq(5)}$$

$$\eta_R{}^B = \frac{4\pi^2}{15}[1.5 + (\frac{\alpha}{\beta})^5]\frac{16}{7}k^3 \quad \text{eq(6)}$$

Disscussion and Conclusion

We found that the stress drop decrease with depth in 90~170 km, whereas the radiated energy scaled by seismic moment declines with depth. As a result, the radiation efficiency exhibit a plateau for events deeper than 90 km. Together these suggest a similar energy dissipation during faulting in ductile deformation regime. It might imply that shear heating instability and dehydration embrittlement as the same important faulting mechanisms for intermediate-depth earthquakes.

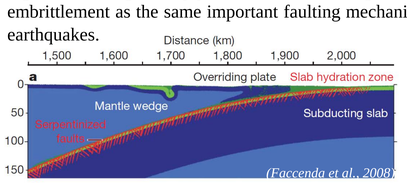

Reference